A Mechanistic Study of Ultrasonically-Enhanced Transdermal Drug Delivery

SAMIR MITRAGOTRI*, DAVID A. EDWARDS*,‡, DANIEL BLANKSCHTEIN*x, AND ROBERT LANGER*x

Received November 16, 1994, from the *Department of Chemical Engineering, Massachusetts Institute of Technology, Cambridge, MA 02139. Accepted for publication February 7, 1995⊗. ‡Present address: Department of Chemical Engineering, The Pennsylvania State University, 158 Fenske Laboratory, University Park, PA 16802.

Abstract □ Although ultrasound has been shown to enhance the transdermal transport of a variety of drugs, the mechanisms underlying this phenomenon are not clearly understood. In this paper, we evaluate the roles played by various ultrasound-related phenomena, including cavitation, thermal effects, generation of convective velocities, and mechanical effects, in the ultrasonic enhancement of transdermal drug delivery (sonophoresis). Our experimental findings suggest that among all the ultrasound-related phenomena evaluated, cavitation plays the dominant role in sonophoresis using therapeutic ultrasound (frequency range, 1–3 MHz; intensity range, 0–2 W/cm^2). Furthermore, confocal microscopy results indicate that cavitation occurs in the keratinocytes of the stratum corneum upon ultrasound exposure. It is hypothesized that oscillations of the cavitation bubbles induce disorder in the stratum corneum lipid bilayers, thereby enhancing transdermal transport. Evidence supporting this hypothesis is presented using skin electrical resistance measurements. Finally, a theoretical model is developed to predict the effect of ultrasound on the transdermal transport of drugs. The model predicts that sonophoretic enhancement depends most directly on the passive permeant diffusion coefficient, rather than on the permeability coefficient through the skin. Specifically, permeants passively diffusing through the skin at a relatively slow rate are expected to be preferentially enhanced by ultrasound. The experimentally measured sonophoretic transdermal transport enhancement for seven permeants, including estradiol, testosterone, progesterone, corticosterone, benzene, butanol, and caffeine, agree quantitatively with the model predictions. These experimental and theoretical findings provide quantitative guidelines for estimating the efficacy of sonophoresis in enhancing transdermal drug delivery.

Transdermal drug delivery offers several advantages over traditional drug delivery methods such as oral delivery and injection. Specifically, transdermal drug delivery (*i*) avoids the passage of drugs through the stomach and the intestine, (*ii*) offers better patient compliance, and (*iii*) provides sustained release of drugs over a sufficiently long time (up to a week). Transdermal drug delivery, however, suffers from the severe limitation that the permeability of the skin to drugs is very low.[1] Consequently, it is difficult to deliver most drugs across the skin at a sufficiently high rate to achieve therapeutically significant drug concentrations in the blood. This is the main reason why only nine drugs are currently administered transdermally for clinical applications. The enormous barrier properties of the skin are attributed to the stratum corneum (SC), the outermost layer of the skin. The SC consists of disk-like dead cells (keratinocytes) containing keratin fibers and water, surrounded by densely packed lipid bilayers.[2] The highly ordered structure of the lipid bilayers confers a highly impermeable character to the SC.[3] A variety of approaches utilizing chemical enhancers and electricity have been proposed to enhance the SC permeability.[4–6] We and others have demonstrated that application of ultrasound can also enhance the transdermal transport of drugs, a phenomenon referred to as sonophoresis.[7–14]

⊗ Abstract published in *Advance ACS Abstracts,* April 15, 1995.

Although significant attention has been devoted to the investigation of sonophoresis in recent years, its mechanisms are not clearly understood. This lack of understanding reflects the fact that several phenomena may occur in the skin upon ultrasound exposure. These include: (*i*) cavitation (generation and oscillation of gas bubbles), (*ii*) thermal effects (temperature increase), (*iii*) induction of convective transport, and (*iv*) mechanical effects (occurrence of stresses due to pressure variations induced by ultrasound). Accordingly, if one can identify the dominant phenomena responsible for sonophoresis, a better selection of ultrasound parameters and the surrounding physicochemical conditions (for example, the solvent in which the drug is dissolved) can be made to selectively enhance the favorable phenomena and hence enhance the efficacy of sonophoresis. This enhancement may greatly assist in broadening the types of drugs that can be administered transdermally.

Although previous investigations of sonophoresis have proposed a number of hypotheses for the possible mechanisms of sonophoresis, no conclusion has been reached. The proposed hypotheses are based on two possibilities: (*i*) ultrasound causes structural changes in the SC,[9–11,14] and (*ii*) ultrasound induces convective transport through hair follicles and sweat ducts of the skin.[12] However, little evidence has been presented to support either hypothesis. Furthermore, the origin and nature of the proposed ultrasound-induced structural changes in the SC are not clear.

In this paper, we present the results of experiments performed to evaluate the roles played by various ultrasound-related phenomena in sonophoresis under therapeutic ultrasound conditions (frequency range, 1−3 MHz; intensity range, 0−2 W/cm^2), the most commonly used ultrasound conditions. Our findings suggest that cavitation plays an important role in sonophoresis. We use the results of confocal microscopy to show that cavitation occurs in the keratinocytes of the stratum corneum. Conclusions concerning the mechanisms of sonophoresis are discussed, and a theoretical model of sonophoresis based on the mechanistic understanding developed in this paper is presented. The predictions of this model, particularly, the dependence of the ultrasound-enhancement of transdermal transport on the permeant characteristics (including passive diffusion coefficient and partition coefficient), are shown to agree quantitatively with the experimental observations of sonophoretic enhancement of seven different permeants.

Experimental Section

Materials—All the permeants studied, including estradiol, progesterone, testosterone, benzene, butanol, caffeine, and corticosterone, were radiolabeled (either tritium or carbon-14; NEN Research Products). Transport experiments were performed with heat-stripped human cadaver skin (male and/or female abdominal or back skin obtained from local hospitals). Heat stripping was performed by keeping full-thickness skin in water at 60 °C for 2 min and then removing the epidermis. The skin was then stored up to 7 days in a chamber at 4 °C and 95% relative humidity until the experiments were performed.

Transdermal Transport Measurements—A section of heat-stripped skin was removed from the chamber just prior to the

0022-3549/95/3184-0697$09.00/0

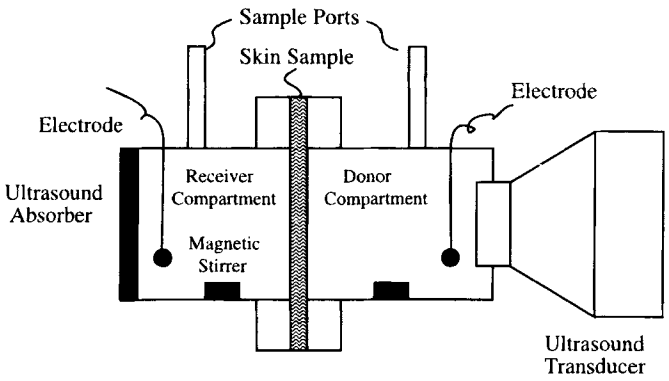

Figure 1—Experimental setup used in the sonophoresis experiments. The donor compartment volume was 8 mL, the receiver compartment volume was 8.5 mL, and the skin diffusion area was 3.14 cm^2.

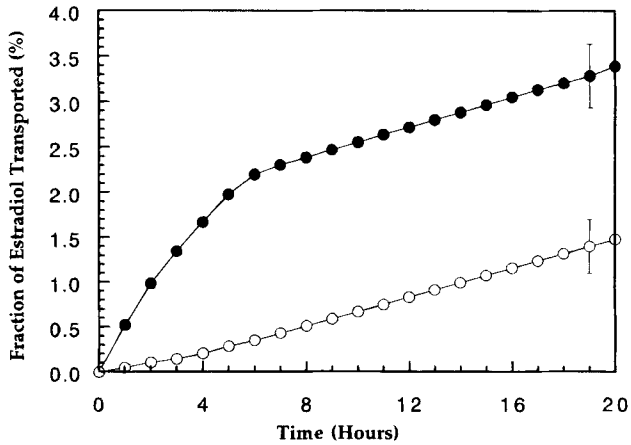

Figure 2—Variation of the transdermal estradiol flux with time during ultrasound exposure (1 MHz, 2 W/cm^2). Key: (●) in the presence of ultrasound; (○) in the absence of ultrasound (passive controls). Typical error bars (SD) are shown on one data point.

experiment and mounted onto a diffusion cell (custom-made with parts manufactured from Crown Glass Company), with the stratum corneum side facing the donor compartment (see Figure 1). The donor compartment was modified to accommodate the ultrasound transducer, and the receiver compartment was modified by replacing its end with a Teflon sheet (1 mm thickness) to absorb ultrasound and thereby minimize the multiple ultrasound reflections in the diffusion cell (see Figure 1). Temperature in the diffusion cell was measured periodically with a thermocouple (VWR Scientific) on the skin surface as well as at other locations close to the skin in the diffusion cell. No spatial variation of temperature was detected. All experiments were performed at room temperature (25 °C). The donor and receiver compartments were clamped together, and the receiver compartment was filled with phosphate-buffered saline (PBS; phosphate concentration, 0.01 M; NaCl concentration, 0.137 M); Sigma Chemical Company). The donor compartment was typically filled with a 1-μCi/mL solution of the permeant in PBS. The concentration of the permeant in the receiver compartment was measured with a scintillation counter (model 2000 CA, Packard). The diffusion cell compartments were stirred with a magnetic stirrer at a speed of 100 rpm. A preliminary calculation,[15] based on the measured skin permeability coefficient and the estimated diffusion coefficient of the permeant in PBS, suggested that for all the permeants, except benzene, the rate-limiting step in the permeant transport from the donor to the receiver compartment is always diffusion though the skin. In other words, the boundary-layer (the unstirred layer close to the skin) transport resistance is always negligible. However, in the case of benzene, the transdermal transport rate is so high (measured skin permeability coefficient of 0.2 cm/h) that a stirring speed of 800 rpm was required to eliminate the boundary-layer transport limitation.

Ultrasound Application—Ultrasound was applied at frequencies of 1 or 3 MHz, and intensities of up to 2 W/cm^2 using an ultrasound generator (model Sonopuls 474, Henley International). The application of ultrasound was always continuous, rather than pulsed, unless mentioned otherwise. The transdermal flux in the presence of ultrasound was measured every hour. Both the donor and the receiver solutions were removed after 4 h, aerated by bubbling air through the solutions, and placed back into the corresponding compartments. This procedure was followed to ensure a sufficiently high dissolved air concentration in the solutions. As will be discussed later, the transdermal flux in the presence of ultrasound decreases with time even though ultrasound is kept continuously on. We found that aerating the donor and receiver solutions every 4 h maintains the transdermal flux at a steady value, which we refer to as the steady-state transdermal flux. The skin permeabilities in the presence of ultrasound, K_p^{us}, as well as those in the absence of ultrasound (passive permeability), K_p^p, were calculated from the steady-state transport rate in the presence and absence of ultrasound, respectively [$K_p = J/\Delta C$, where J is the steady-state transdermal flux and ΔC is the concentration difference across the skin]. The enhancement ratio, E, for a given permeant is defined as the ratio of K_p^{us} and K_p^p; that is, $E = K_p^{us}/K_p^p$. The intensity of ultrasound on the skin surface was measured with a hydrophone (model PZT 54, Specialty Engineering Associates) that was coupled to a hydrophone preamplifier (model A17DB, Specialty Engineering Associates) and finally connected to an oscilloscope (model 7623 A, Hewlett Packard). The hydrophone was calibrated by Sonic Technologies.

Electrical Resistance Measurements—The Ag/AgCl electrodes (E242, Invivo Metrics) were introduced in the donor and receiver compartments to measure the skin electrical resistance (see Figure 1). The skin electrical resistance was measured every 15 min, before, during, and after the ultrasound exposure. To measure the skin electrical resistance, an AC electrical field, typically at 50 mV and 10 Hz, was applied across the electrodes for a short time (typically, for 5 s) with a signal generator (model HP 4116 A, Hewlett Packard). The electric current through the skin was then measured with an ammeter (Texas Instruments), and the electrical resistance was calculated by Ohm's law. The saline resistance was measured separately with the same assembly, but without mounting the skin. The measured skin resistance is the sum of the actual skin resistance and the saline resistance, so the latter was subtracted from the measured skin resistance to obtain the actual skin resistance.

Confocal Microscopy—Confocal microscopy allows the optical cross-sectioning of a sample (for example, the SC) by deconvoluting fluorescence from various depths in the sample. This technique allows a better visualization of the inner layers of the SC. Skin samples to be observed under the confocal microscope were frozen immediately after the sonophoresis experiment (details of these experiments are discussed later). These samples were defrosted prior to the microscopic observations, mounted on a microscopic slide as flat as possible, and placed under a confocal microscope (model MRC-600, Bio-Rad). The samples were excited with a Krypton-Argon laser beam at a wavelength of 488 nm, and the emitted light signals were analyzed at a wavelength of 515 nm to generate a digitized micrograph.

Results and Discussion

Ultrasound Enhances Transdermal Transport of Drugs—Continuous application of ultrasound at 1 MHz and 2 W/cm^2 enhanced the transdermal transport of a variety of permeants. For example, a comparison of the cumulative amount of estradiol transported transdermally in the presence and absence of ultrasound (control) is shown in Figure 2. The transport rate (flux) in both cases is proportional to the slopes of the corresponding curves. The control transdermal flux attains a steady value (indicated by a constant slope of the curve) within 1 h of beginning the experiment. On the other hand, the transdermal flux in the presence of ultrasound exhibits a significant temporal variation. Initially, it is 13-fold higher than that of the control, and remains at this value for ~4 h. However, continued application of ultrasound after this initial 4-h period has a progressively smaller enhancement effect and, eventually (typically, after 6 h), the transdermal estradiol flux in the presence of ultrasound becomes comparable to the control flux (the slopes of the two curves are equal).

Table 1—Summary of the Observed Enhancement of Transdermal Transport Due To Ultrasound Exposure

Permeant	Molecular Weight (Da)	Passive Permeability,[a] K_p (cm/h)	Partition Coefficient (Octanol/Water), $K_{o/w}$	Passive Diffusivity, D_o (cm²/s)[b]	Bulk Diffusivity, D^∞ (cm²/s)[c]	Ultrasound Enhancement, E
Benzene	78	1.6×10^{-1}	100[d]	2.6×10^{-5}	2×10^{-6}	1 ± 0.2
Butanol	162	2.2×10^{-3}	7.5[d]	2.5×10^{-6}	2×10^{-6}	1.5 ± 0.5
Caffeine	194	1.0×10^{-4}	1[d]	3.4×10^{-6}	1×10^{-6}	1.2 ± 0.4
Corticosterone	346	3.0×10^{-4}	87[d]	5.4×10^{-8}	1×10^{-6}	4 ± 0.6
Estradiol	272	3.2×10^{-3}	7000[e]	2.0×10^{-8}	1×10^{-6}	13 ± 1.5
Progesterone	274	1.3×10^{-2}	6000[d]	9.8×10^{-8}	1×10^{-6}	1 ± 0.5
Testosterone	288	2.2×10^{-3}	2070[e]	3.8×10^{-8}	1×10^{-6}	5 ± 1.1

NOTE: Some of the relevant molecular properties of the permeants are also listed. [a] Measured by the authors. [b] Estimated by methods described in ref 32 after substituting[e] $K_m = K_{o/w}^{0.75}$. [c] Estimated with the Wilke–Chang equation given in ref 37. [d] Hanch, C.; Leo, A. In *Substituent Constants for Correlation Analysis in Chemistry and Biological Sciences*; Wiley: New York, 1979. [e] Johnson, M. E., unpublished data.

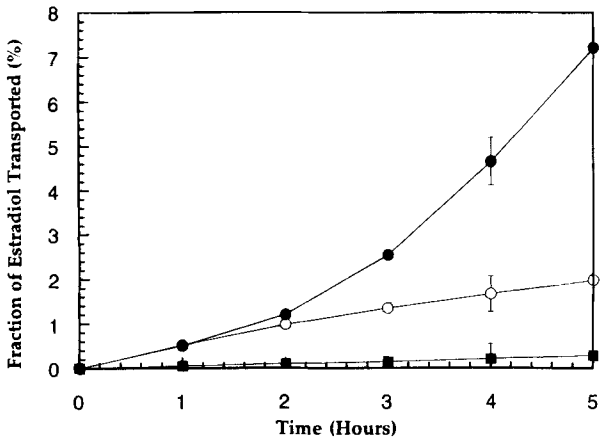

Figure 3—Effect of repeated aerating on the transdermal flux of estradiol in the presence of ultrasound (1 MHz, 2 W/cm²). Key: (●) donor solution aerated every hour, (○) no repeated aerating; (■) passive controls. Typical error (SD) bars are shown on one data point.

A plausible explanation for the observed reduction in the ultrasound efficacy to enhance transdermal transport is that ultrasound causes degassing of the saline surrounding the skin due to cavitation.[16] Dissolved air is necessary for cavitation, so a decrease in the dissolved air concentration in the saline may cause a decrease in the cavitation activity. To check the hypothesis that reduced air content in the donor compartment solution reduces cavitation activity and hence ultrasound efficacy, we performed additional sonophoresis experiments in which we removed the donor and receiver solutions every hour, bubbled air through these solutions for 5 min, and then put them back in their corresponding compartments. Results of these experiments are shown in Figure 3. The transdermal flux in the presence of ultrasound when the solutions are aerated every hour remains high, well beyond the initial 4-h period, in contrast to the leveling off when the solutions are not aerated repeatedly. In fact, the observed flux increases after every aeration. We also found that whereas aerating every hour continuously increases the transdermal flux, aeration every 4 h maintains the transdermal flux at a steady value. Accordingly, we aerated the donor and receiver solutions every 4 h in all subsequent experiments. The observation that dissolved air content in the donor and receiver solutions plays an important role in the efficacy of ultrasound in enhancing transdermal transport suggests that *cavitation may play a major role in sonophoresis*.

A prolonged ultrasound exposure of the skin may cause a significant temperature increase, so we continuously monitored the diffusion cell temperature. The diffusion cell temperature increased by ~7 °C during the first 0.5 h of exposure to ultrasound, and then remained constant at 32 °C (note that the initial temperature was 25 °C). The importance of this temperature increase in the observed enhancement is discussed later.

We also found that ultrasound under similar conditions enhances transdermal transport of a variety of other permeants, including testosterone, benzene, corticosterone, progesterone, caffeine, and butanol, to an extent that depends on the physicochemical properties of the permeant. The molecular properties and the corresponding ultrasound-mediated transdermal transport enhancements of these permeants are listed in Table 1. A detailed discussion of the dependence of sonophoresis on molecular properties is presented later. In our subsequent experiments which were conducted to analyze the importance of each mechanism, we chose estradiol as a model permeant because of all the permeants studied, estradiol transdermal transport showed the highest enhancement in the presence of ultrasound (see Table 1). We also performed several experiments with permeants other than estradiol (e.g., testosterone) to verify the generality of our findings.

Possible Mechanisms of Sonophoresis—Many phenomena, including cavitation, thermal effects, generation of convective velocities, and mechanical effects, have been considered to play a role in the ultrasound-mediated enhancement of transdermal transport. We present here a detailed description of the possible role played by each of the mechanisms and the experiments performed to elucidate the relative importance of each mechanism in sonophoresis.

Cavitation—Cavitation involves the generation and oscillation of gaseous bubbles in a medium, and may be induced by the exposure to ultrasound. Cavitation occurs due to the nucleation of small gaseous cavities during the negative pressure cycles of ultrasound, followed by the growth of these bubbles throughout subsequent pressure cycles.[17] It is noteworthy that whenever small gaseous nuclei already exist in a medium, cavitation takes place preferentially at those nuclei.[18]

The minimum ultrasound intensity required for the onset of cavitation, referred to as the *cavitation threshold*, increases rapidly with ultrasound frequency. No significant cavitational effects have been observed in *fluids* at high ultrasound frequencies (frequency > 2.5 MHz), even at intensities that are much higher than those corresponding to therapeutic ultrasound.[19] As a result, 2.5 MHz is considered to be a reasonable estimate of the upper frequency limit for the occurrence of cavitation in fluids at therapeutic ultrasound intensities. The cavitation threshold also depends significantly on the ultrasound pulse length. For example, the cavitation threshold in an aqueous solution at 1 MHz changes from ~0.3 W/cm² [20] to 33 W/cm² [21] as the mode of ultrasound application changes from continuous to pulsed, with a pulse length of 1 ms applied every 10 ms.

We performed experiments to determine if the dependence of sonophoresis on ultrasound frequency and pulse length follows a trend similar to that of the cavitation activity in fluid media. The results of these experiments are presented in

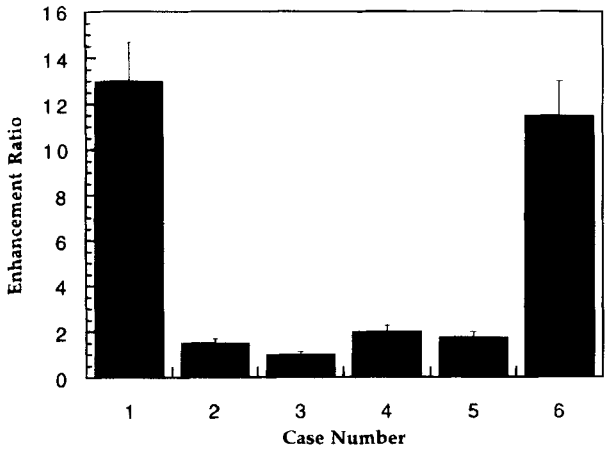

Figure 4—Effect of ultrasound on the transdermal estradiol transport under a variety of conditions. Key: (**case 1**) 1 MHz from normal buffer; (**case 2**) 3 MHz from normal buffer; (**case 3**) 2 ms pulsed application from normal buffer; (**case 4**) 1 MHz compressed skin; (**case 5**) 1 MHz deaerated skin; (**case 6**) 1 MHz form viscous solvent. Cases 2, 3, 4, and 5 suggest that cavitation in the skin plays a major role in sonophoresis, whereas case 6 suggests that cavitation outside the skin does not play any role in sonophoresis.

Figure 4, and may be used to test the hypothesis that cavitation is a possible mechanism of sonophoresis. Whereas 1 MHz ultrasound (2 W/cm^2, continuous) resulted in a 13-fold enhancement of the transdermal estradiol flux, 3 MHz ultrasound (2 W/cm^2, continuous) resulted in only a 50% enhancement (compare cases 1 and 2 in Figure 4). Furthermore, application of 2-ms ultrasound pulses (one pulse every 10 ms) at 2 W/cm^2 and 1 MHz did not cause any enhancement of estradiol transdermal transport (see case 3 in Figure 4). These results are consistent with the aforementioned dependence of cavitation in fluids on ultrasound parameters, and indicate that *cavitation may play an important role in the observed ultrasound-mediated transdermal transport enhancement.*

Cavitation may occur either inside the skin (in particular, inside the SC), outside the skin, or in both domains. Accordingly, we examined each possibility in detail as described below.

Cavitation Inside the Skin as a Possible Sonophoresis Mechanism—Cavitation occurs in a variety of mammalian tissues, including muscle, abdominal tissues, brain, cardiovascular tissues, and liver, upon exposure to ultrasound at a variety of conditions that include the aforementioned therapeutic range.[20] As explained earlier, the occurrence of cavitation in biological tissues is attributed to the existence of a large number of gas nuclei. These nuclei are gas pockets trapped in either intra- or intercellular structures. To determine whether cavitation occurs inside the skin, we performed two sets of experiments.

In the first set, we utilized the known effect of static pressure on cavitation, that is, cavitation in fluids and porous media[22] can be suppressed at high pressures. This effect is believed to occur because of the dissolution or collapse of the gaseous nuclei under the influence of pressure. Based on this known effect, we designed experiments in which pieces of heat-stripped human cadaver skin were compressed prior to the sonophoresis experiment. This compression was achieved by placing the skin pieces between two smooth glass plates soaked in water, and then compressing the entire assembly with a compression press at a pressure of 30 atm for 2 h. The skin pieces were then removed, and permeability experiments were performed according to the protocols described before. We also performed control experiments on compressed skin and found that compression reduces the control flux by 50% compared with normal controls. When the compressed skin piece was exposed to ultrasound (1 MHz, 2 W/cm^2), the transdermal transport was enhanced only by 75% in contrast to the 13-fold increase found in the case of uncompressed skin (compare cases 1 and 4 in Figure 4; note that the control flux used to calculate the enhancement ratio in case 4 was also measured using compressed skin).

In the second set of experiments, we deaerated heat-stripped human cadaver skin prior to the permeability experiments. We anticipated that when a skin piece soaked in buffer is subjected to high vacuum, the resulting low pressures should reduce the dissolved gas concentration in the buffer, thereby forcing small gaseous nuclei in the skin to dissolve. Deaerating of the skin was achieved by placing the skin in buffer and maintaining a 0.05 mmHg over it for 2 h. After this was done, the skin was removed and permeability experiments were performed according to the protocols described in the section entitled *Ultrasound Application*. Control fluxes were also measured in deaerated skin, and were ~40% higher than those corresponding to the normal control fluxes. This higher flux probably occurs because of structural changes in the SC lipid bilayers in skin exposed to high vacuum. When the deaerated skin was exposed to ultrasound, once again, the effect of ultrasound on the permeability of deaerated skin was minimal (50%). These results support the hypothesis that *cavitation inside the skin plays a major role in enhancing transdermal transport upon ultrasound exposure* (see case 5 in Figure 4; note that the control flux used to calculate the enhancement ratio was also measured with deaerated skin).

The occurrence of cavitation inside the skin was investigated further, with emphasis on its location within the skin (SC, in particular) as well as its effect on transdermal transport. The results of these investigations are discussed in the section entitled *Location of Cavitation Inside the SC.*

Cavitation Outside the Skin as a Possible Sonophoresis Mechanism—We performed experiments to assess the importance of cavitation outside the skin. Cavitation in the saline surrounding the skin does occur after ultrasound exposure. Indeed, the resulting cavitation bubbles can be seen by the naked eye. These cavitation bubbles can potentially play a role in the observed enhancement of the transdermal transport in a number of ways. First, these bubbles may cause skin erosion following their violent collapse on the skin surface due to the generation of shock waves,[23] thereby enhancing transdermal transport. Second, the oscillations and collapse of cavitation bubbles may also cause generation of velocity jets at the skin–donor solution interface. This phenomenon is referred to as microstreaming[24] and may induce convective transport across the skin, thereby enhancing the overall transdermal transport.

To assess the importance of cavitation outside the skin, we utilized the well-known fact that cavitation activity in a fluid medium decreases as the viscosity of the medium increases. This change probably occurs because of a decrease in the ability of gases to diffuse from the bulk fluid to the nucleation sites.[25] We studied the effect of ultrasound on the transdermal flux of a permeant from two different donor solutions. In the first case, the donor solution consisted of estradiol in PBS (viscosity of ~0.9 cP). In the second case, the donor solution consisted of estradiol in a water-soluble viscous gel (Polyfreez, Polyscience, viscosity of >100 cP). The receiver compartment was filled with PBS in both cases. Ultrasound (1 MHz, 2 W/cm^2) was applied as described in the *Experimental Section.* Control experiments indicated that the passive transdermal transport rate is not affected by the fact that the donor solution viscosity is high. This result is plausible because the rate-limiting step in permeant transport from the donor compartment to the receiver compartment is always the

diffusion through the skin and not the diffusion in the donor compartment. Upon ultrasound exposure, *we did not observe any cavitation bubbles in the gel*; these bubbles are otherwise clearly visible if the donor compartment contains an estradiol solution in PBS. Nevertheless, the ultrasound-induced transdermal transport enhancement in this case was *comparable* to that when the donor compartment contains estradiol solution in PBS (compare cases 1 and 6 in Figure 4). This finding suggests that *cavitation outside the skin may not play an important role in sonophoresis with the ultrasound conditions examined.*

Thermal Effects—The increase in the skin temperature resulting from the absorbance of ultrasound energy may increase the skin permeability coefficient because of an increase in the permeant diffusion coefficient. In a different set of experiments, we found that a temperature increase of 10 °C causes about a two-fold increase in the estradiol skin permeability (data not shown). This observation is also in agreement with the literature reports[26] suggesting about a two-fold increase in the skin permeability coefficient per 10 °C rise in the skin temperature. Because the typical skin temperature increase in our sonophoresis experiments is ~7 °C, we conclude that *thermal effects cannot explain the observed 13-fold enhancement of estradiol transdermal transport upon ultrasound exposure.*

Role of Convective Transport in Sonophoresis—Fluid velocities are generated in a porous medium exposed to ultrasound for a variety of reasons, including the interference of the incident and reflected ultrasound waves in the diffusion cell and oscillations of the cavitation bubbles. Fluid velocities generated in this way may affect transdermal transport by inducing convective transport of the permeant across the skin, especially through hair follicles and sweat ducts. To assess the validity of this hypothesis, we performed electrical resistance measurements of the skin exposed to ultrasound. The mobility of ions in the skin is sufficiently high that the electrical resistance measured with moderate electric fields constitutes an almost instantaneous indicator of the skin transport properties.[27] In addition, the time required to establish convective currents in the donor compartment or in the follicles (hair follicles and sweat ducts) of the skin (both filled with buffer) upon ultrasound exposure is expected to be fairly short (of the order of seconds) due to the low viscosity of water.[28] Accordingly, if exposure to ultrasound changes the skin electrical resistance and if convective transport plays an important role in sonophoresis, we expect to observe a rapid change in the skin electrical resistance. A typical measured variation of electrical resistance, R (normalized by the initial resistance, R_o), of the skin with time upon ultrasound application (1 MHz, 2 W/cm^2) is shown in Figure 5. Results from a single, typical experiment are shown to clearly depict the shape of the curve. The electrical resistance of the skin decreases upon ultrasound exposure due to increased ionic mobility. As shown in Figure 5, the electrical resistance decreases by ~30% over a period of 45 min. The decrease is nearly exponential and far from rapid, suggesting that *convective transport does not play an important role in the observed enhancement.* The significance of the observed 30% decrease in the skin electrical resistance is discussed later.

Role of Mechanical Stresses in Sonophoresis—Ultrasound is a longitudinal pressure wave inducing sinusoidal pressure variations in the skin. Nevertheless, there is no significant net pressure gradient across the SC at any time because the thickness of the SC (15 μm) is very small compared with a typical ultrasound wavelength (1500 μm at 1 MHz). The sinusoidal pressure variations induce sinusoidal density variations in the medium. At low ultrasound frequencies, these density variations can grow into a gas or vapor bubble, thus giving rise to cavitation. However, at higher frequencies,

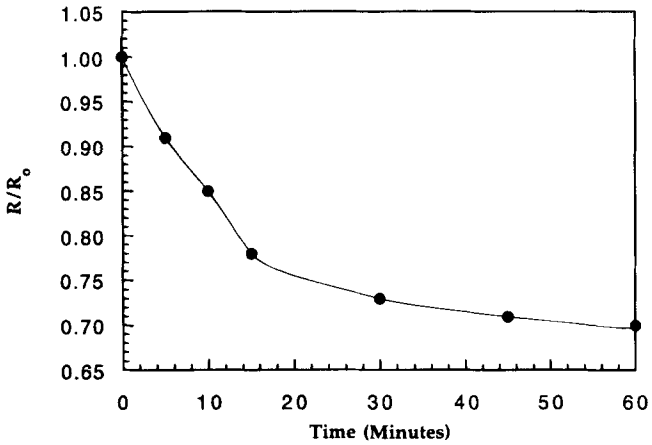

Figure 5—Variation of the electrical resistance, R, of the skin (normalized by the initial resistance, R_o) with time upon ultrasound exposure.

where the density variations occur so rapidly that a small gaseous nucleus cannot grow, cavitational effects cease, although other effects due to density variations may continue to occur. These effects include primarily the generation of cyclic stresses due to density changes that ultimately lead to fatigue of the medium. Lipid bilayers, being self-assembled structures, can easily be disordered by these stresses, which results in an increase in the bilayer permeability.

The hypothesis that mechanical stresses play an important role in the therapeutic ultrasound range is inconsistent with the previously mentioned observation that the effect of 1 MHz ultrasound on transdermal transport decreases with time due to deaerating of the solutions in the diffusion cell (see Figure 2), because the mechanical effects continue to occur in the skin even though the surrounding solution is deaerated. In addition, it is known from investigations of the effect of cyclic stresses on polymers and metals, that the mechanical effects are proportional to the stress frequency.[29] Because the frequency of cyclic stresses (if any) in a medium exposed to ultrasound follows the ultrasound frequency, one would expect that if mechanical effects play a major role in sonophoresis, ultrasound at higher frequencies should be at least equally efficacious in enhancing transdermal transport. However, we found that 1 MHz ultrasound enhanced estradiol transdermal transport by a factor of 13, whereas 3 MHz ultrasound enhanced transport only by 50% (compare cases 1 and 2 in Figure 4). These observations suggest that *mechanical effects do not play an important role in sonophoresis with ultrasound in the therapeutic frequency range.* However, it should be noted that the mechanical effects could become increasingly important in the high-frequency range (frequency > 3 MHz).

The experimental findings described in this section suggest that *among all the possible mechanisms of sonophoresis, cavitation inside the skin (most likely, inside the SC) is the dominant one.* In the next section, we discuss the results of additional experiments designed to elucidate the location of cavitation inside the SC.

Location of Cavitation Inside the SC—A schematic, multiscale representation of a cross-section of the skin is shown in Figure 6. The three principal layers of the skin, namely, the SC, the epidermis, and the dermis are shown in Figure 6A. As explained earlier, the SC comprises densely packed disk-like keratinocytes separated by multilamellar lipid bilayers (see Figure 6B). The keratinocytes, which are ~50% water-filled (by volume), possess a lateral dimension of ~23 μm and a longitudinal dimension of ~1 μm.[30] The lamellar bilayer zones separating the keratinocytes are ~0.05 μm (50 nm) in thickness and possess a small amount of bound water.[2] Typically, the lamellar lipid region between two keratinocytes consists of 10 lipid bilayers (see Figure 6C).

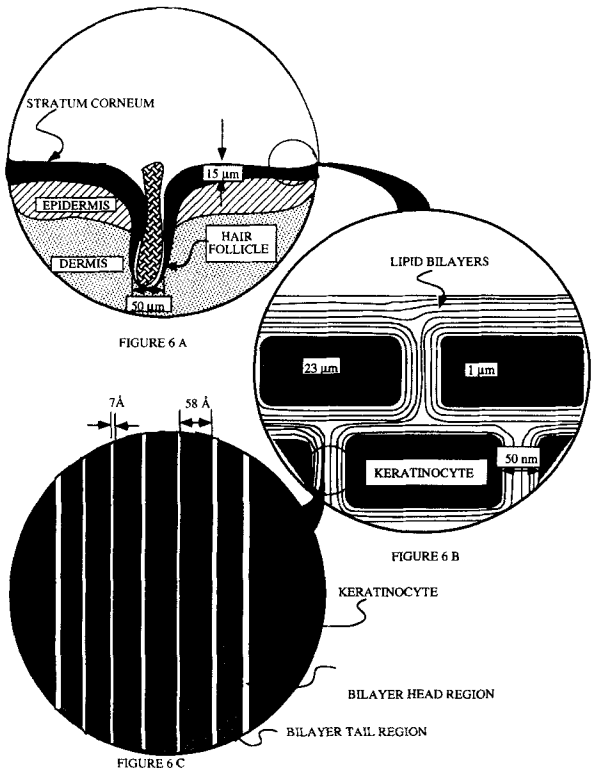

Figure 6—Schematic sketch of various transdermal transport pathways. The major transport pathway comprises the intercellular lipid bilayers. Figure 6A shows three principal layers of the skin; that is, the SC, the epidermis, and the dermis. A section of the SC is blown up in Figure 6B. Figure 6C shows details of the intercellular lipid bilayers.

Cavitation inside the SC can potentially take place in the keratinocytes or in the lipid regions or in both. As described earlier, the effect of ultrasound on transdermal transport depends strongly on the dissolved air content in the surrounding buffer. It should be noted that a reduction in the dissolved air concentration in the surrounding buffer may also reduce the gas concentration inside the SC, because of rapid diffusion of air though the skin lipids, and thereby reduce cavitation inside the skin. Because dissolved air present in the surrounding buffer plays an important role in sonophoresis and because most of the water in the SC is present in the keratinocytes,[30] we hypothesize that *cavitation inside the SC may take place in the keratinocytes*. Accordingly, we performed experiments to verify the validity of this hypothesis.

It has long been known that cavitation in an aqueous medium leads to the formation of hydroxyl radicals after adiabatic collapse of the cavitation bubbles.[31] The hydroxyl radicals, being very unstable, react with water to from hydrogen peroxide, a strong oxidizing agent. In a different set of experiments, we found that hydrogen peroxide oxidizes fluorescein, a highly fluorescent dye, into a nonfluorescing compound (data not shown). On the basis of this observation and the fact that ultrasound exposure in water leads to the formation of hydrogen peroxide, we expected that an exposure to ultrasound should result in a significant bleaching of fluorescein. Indeed, as can be seen in Figure 7, a significant amount of fluorescein is bleached upon continuous exposure of its aqueous solution (1 μg/mL) to ultrasound (1 MHz, 2 W/cm^2). The initial rate of bleaching is high, although it decreases with time. This decrease is probably due to reduced cavitation activity. We also found that 3 MHz ultrasound at the same intensity does not induce any bleaching (data not shown). This result suggested that bleaching in the presence of ultrasound was related to cavitational effects. Therefore, we anticipated that if significant cavitation activity occurs in

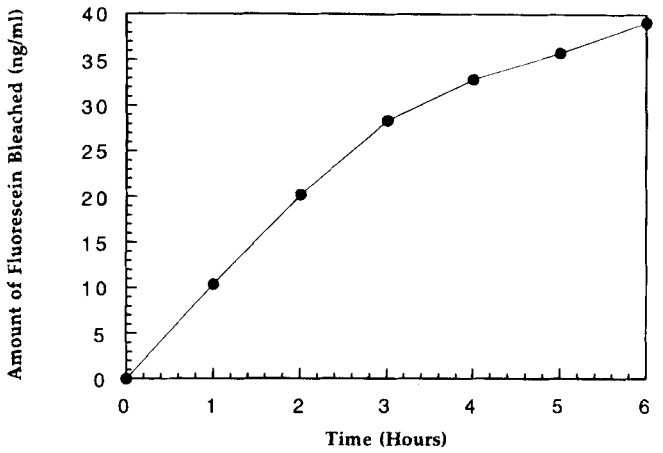

Figure 7—Variation of the amount of fluorescein bleached as a function of the ultrasound exposure time. This bleaching occurs because of oxidation of fluorescein by cavitation-generated peroxide radicals. Results from a single experiment are shown to depict the shape of the curve clearly. The typical error (SD) in the data is 15%.

the SC upon ultrasound exposure, we should see a similar bleaching of the fluorescence in SC preloaded with fluorescein.

We soaked heat-stripped human cadaver skin in a 1-μg/mL solution of fluorescein, and the solution was kept at 4 °C to ensure minimal skin degradation during storage. After 5 days of soaking, we observed these samples with a fluorescent confocal microscope. A typical confocal micrograph revealing the well-known honey-comb like structure of the SC is shown in Figure 8. The hexagonal structures are the keratinocytes and the bright, contiguous borders around the keratinocytes are the intercellular lipid bilayers. Note the presence of fluorescein (proportional to the brightness in the micrograph) in both the keratinocytes and in the intercellular lipid bilayers.

Ultrasound (1 MHz, 2 W/cm^2) was applied to similar skin pieces (soaked in a 1-μg/mL solution of fluorescein) by direct contact between the ultrasound transducer and the fluorescein solution in which the skin pieces were soaking. Ultrasound was turned off after 30 min. The skin pieces were washed and immediately frozen to minimize fluorescein transport after the exposure. Later, we observed these skin pieces with the confocal microscope. The fluorescence in the keratinocytes was significantly bleached, whereas the fluorescence in the intercellular lipids was not seriously affected (see Figure 9). Before concluding that the observed bleaching of fluorescein in the keratinocytes was due to cavitational effects, we considered the possibility that ultrasound caused the transport of fluorescein out of the SC, thereby causing a reduction of fluorescence brightness in the keratinocytes. However, this event is unlikely to occur during a 30-min exposure to ultrasound because the diffusion coefficient of fluorescein in the lipid bilayers is expected to be low (the passive diffusion coefficient of fluorescein is $\sim 5 \times 10^{-10}$ cm^2/s, as estimated from the measured passive permeability coefficient and methods for calculating the diffusion coefficient described in ref 32). Furthermore, the skin was always surrounded by the fluorescein solution with which it was equilibrated for 5 days. Hence, there was no significant concentration gradient across the skin at any time. Accordingly, the loss of fluorescence upon ultrasound exposure can be attributed to the bleaching effect. To confirm that the bleaching was related to cavitational effects, we performed similar experiments with 3 MHz ultrasound (2 W/cm^2), and found that 3 MHz ultrasound did not bleach fluorescein in the skin. *These findings strongly support the hypothesis that ultrasound induces cavitation in the keratinocytes*. However, it should be noted that these

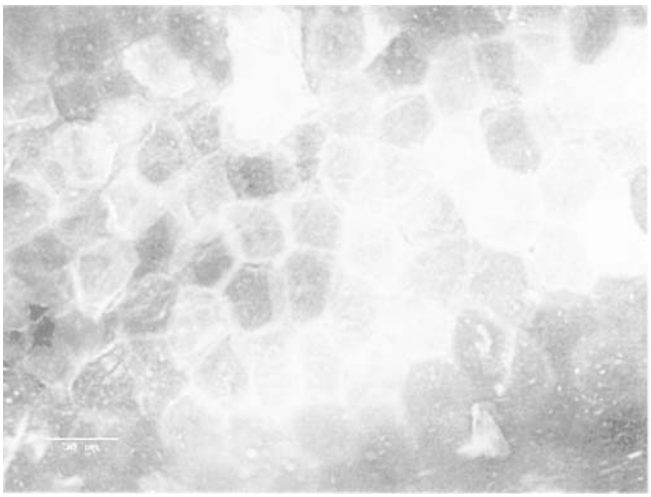

Figure 8—Confocal micrograph of the skin loaded with fluorescein. Note the significant amount of fluorescein in the keratinocytes (proportional to the brightness in the micrograph).

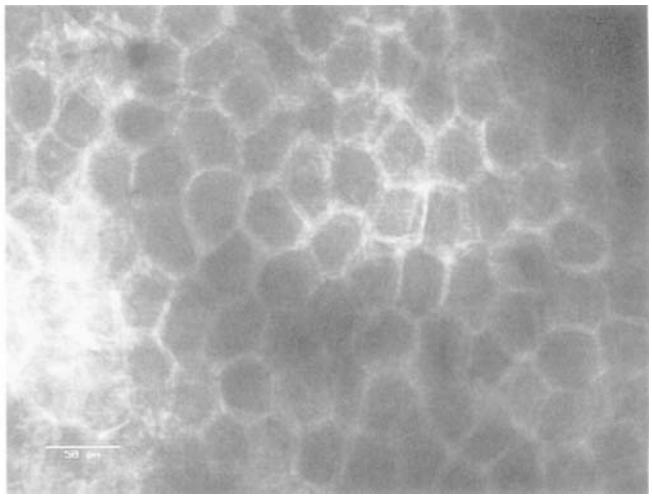

Figure 9—Confocal micrograph of the skin exposed to ultrasound for 30 min. Note that a significant amount of fluorescein in the keratinocytes is bleached, thus suggesting occurrence of cavitation activity in the keratinocytes.

findings do not rule out the possibility of the occurrence of cavitation in the intercellular lipids.

Mechanism of Sonophoresis—Based on the discussions presented in the previous sections, it appears that ultrasound exposure in the therapeutic range causes cavitation in the keratinocytes of the SC. Oscillations of the ultrasound-induced cavitation bubbles near the keratinocyte–lipid bilayer interfaces may, in turn, cause oscillations in the lipid bilayers, thereby causing structural disorder of the SC lipids. Shock waves generated by the collapse of cavitation bubbles at the interfaces may also contribute to the structure-disordering effect. Because the diffusion of permeants through a disordered bilayer phase can be significantly faster than that through a normal bilayer, transdermal transport in the presence of ultrasound is expected to be higher than passive transport. In the next section, we present a quantitative description of sonophoresis based on our proposed mechanism of cavitation-induced bilayer disordering. Additional evidence to support the proposed mechanism is also presented.

Quantitative Model of Sonophoresis—*Basic Transdermal Transport Equations*—The passive skin permeability coefficient, K_p^p, is defined as the ratio of the molecular flux and the concentration difference across a uniform-thickness sample of SC. Under steady-state conditions, K_p^p may be expressed as follows:[32]

$$K_p^p = \bar{K}\left[\frac{\bar{D}^*}{h}\right] \quad (1)$$

where $\bar{K}$ is the *SC–donor solution partition coefficient* of the permeant, $\bar{D}^*$ is the *effective permeant diffusion coefficient in the SC* (cm²/s), and *h is the SC thickness* (15×10^{-4} cm).[2] The passive transdermal transport of permeants occurs mainly through intercellular lipids,[2] so $\bar{K}$ can be related to the partition coefficient of the permeant in the bilayer, K_m, and $\bar{D}^*$ can be related to the permeant diffusion coefficient in the bilayers, D_o, through geometric parameters. These parameters include the fractional skin area occupied by the lipids (estimated value of 0.19%[32]), and the ratio of the average length of the tortuous intercellular pathway to the SC thickness (estimated value of 24[32]). For a detailed discussion of the estimation of these geometric parameters, see ref 32. Substituting characteristic values for the SC geometric parameters in eq 1 and representing K_p^p in units of cm/h (note that the diffusion coefficient units are cm²/s), results in eq 2:

$$K_p^p = 0.0019K_m\left[\frac{D_o \times 3600}{(24) \times (15 \times 10^{-4})}\right] = 194K_mD_o(\text{cm/h}) \quad (2)$$

Similarly, the effective electrical conductivity of the skin, $\bar{\sigma}$, can be described theoretically on the basis of the transport of ions such as sodium and chloride (present in the saline solution around the skin) through the shunt pathways as well as through the intercellular lipids. Specifically, $\bar{\sigma}$ is given by eq 3:[32]

$$\bar{\sigma} = 1.2(1.2 \times 10^{-5} + 2.34 \times 10^{-4}\Phi)\,(\Omega\ \text{m})^{-1} \quad (3)$$

In eq 3, the first term in the brackets represents the contribution of the shunt pathways and the second term represents the ionic motion along the intercellular lipid bilayers. The parameter, Φ, is a function that expresses the hindrance of ionic motion as the ions pass through the confined regions between the head groups of the lipid bilayers of the SC. The value of Φ can be estimated with the analytical results of Faxen *et al.*[33] and Glandt,[34] which describe, respectively, the transport and partitioning of spheres through a narrow rectilinear channel bounded by parallel walls. For unaltered configurations of the SC lipids, the lipid head groups from adjacent bilayers have been observed to be in extremely close proximity (the average bilayer separation is ~7 Å[35]). Under these circumstances, assuming the hydrated radius of an ion such as sodium to be 3 Å, Φ can be estimated[32] to be ~0.08.

Physical Description of Transdermal Transport in the Presence of Ultrasound—As described earlier, exposure to ultrasound gives rise to cavitation in the keratinocytes of the SC. The existence of these cavitation bubbles and their oscillation in the presence of the propagating acoustic wave may cause disordering of the intercellular lipids in the immediate vicinity of the keratinocytes. The intercellular lipid domains of the SC are assumed to be subdivided into regions of ordered lipid bilayers with a fractional thickness of $1 - f$, and disordered lipid regions with a fractional thickness of f. The ionic transport through the disordered lipid bilayer regions is assumed to be essentially unhindered ($\Phi = 1$), and the diffusion coefficient of permeants through this region is assumed to be equal to that in free hydrocarbon, D^∞. The permeant partition coefficient in the bilayer, K_m, is expected to increase upon disordering by less than one order of magnitude.[36] However, because of the cavitation activity, a certain amount of water is expected to penetrate in the disordered lipid regions. This water penetration may lead to

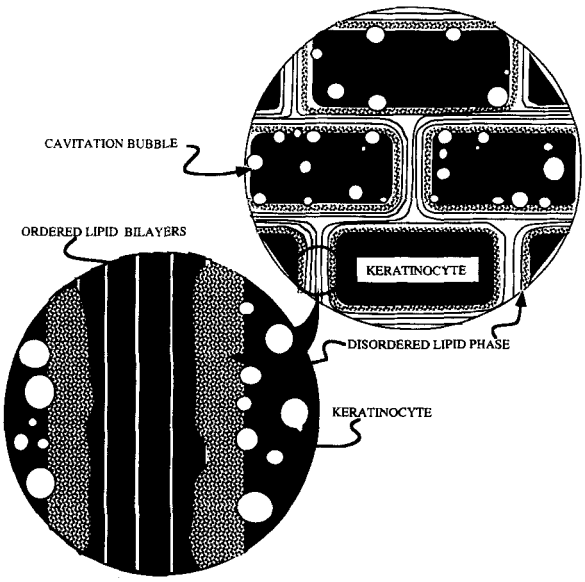

Figure 10—Schematic sketch of cavitation occurring in the keratinocytes. Cavitation occurs preferentially at the interface between the keratinocytes and the lipid bilayers.

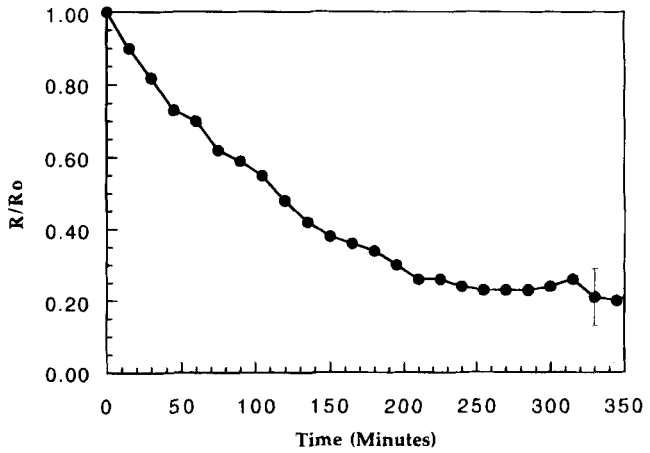

Figure 11—Effect of long-time ultrasound exposure on the skin electrical resistance, R/R_o. The electrical resistance drops after every reaerating (done every hour) and finally levels off at a value of ~0.2 that corresponds to a lowering of the skin resistance by a factor of 5. Typical error bar (SD) is shown on one data point.

a reduction of the partition coefficient of lipophilic molecules in the disordered bilayers. Because of these two opposing effects, the partition coefficient of the permeant in the bilayers may not change significantly upon bilayer disordering. In addition, as will be shown later, the permeant diffusion coefficients in an intact bilayer, D_o, and that in a disordered bilayer, D^∞, typically differ by a few orders of magnitude. Hence, the effect of bilayer disordering on the drug diffusion coefficient is much larger than the possible effect on the partition coefficient. Therefore, in this analysis, we do not account for the change in the permeant partition coefficient upon bilayer disordering.

Mathematical Description of Sonophoresis—Based on the model of ultrasound-induced lipid bilayer disordering just presented (see also Figure 10), eqs 2 and 3 can be expressed as follows:

$$K_P^{us} = 194K_m[fD^\infty + (1-f)D_o]\,(\text{cm/h}) \tag{4}$$

$$\bar{\sigma}^{\mu s} = 1.2[1.2 \times 10^{-5} + 2.34 \times 10^{-4}(f + (1-f)\Phi]\,(\Omega\text{m})^{-1} \tag{5}$$

Equation 4 describes the skin permeability coefficient to permeants in the presence of ultrasound, and eq 5 represents the corresponding skin electrical conductance. Dividing eq 4 by eq 2 and eq 3 by eq 5 yields the following expressions for the permeability enhancement ratio in the presence of ultrasound, E, and for the electrical resistance reduction ratio, R/R_o:

$$E \equiv \frac{K_p^{us}}{K_p^p} = 1 + f\left[\frac{D^\infty}{D_o} - 1\right] \tag{6}$$

$$\frac{R}{R_o} \equiv \frac{\bar{\sigma}}{\bar{\sigma}^{\mu s}} = \frac{2.81}{1 + 19.5[f + 0.08(1-f)]} \tag{7}$$

Equations 6 and 7 are simple analytical expressions that may be used to predict the transdermal permeability enhancement and the transdermal resistance drop in the presence of therapeutic ultrasound as a function of the transport properties of the permeant under consideration. These predictions require knowledge of the transport coefficients, D_o and D^∞, as well as of the fractional thickness of the lipid region disordered due to ultrasound application, f. The lateral passive diffusion coefficient, D_o, of the permeant through the SC intercellular lipids may be deduced from eq 1 by measurement of the passive transdermal permeability coefficient and a knowledge of the permeant partition coefficient in lipids, K_m (see the footnote to Table 1 for a discussion of methods for the estimation of K_m). The bulk diffusion coefficient, D^∞, can be measured in a representative alkane (for example, octane) or estimated on the basis of an established empirical formula.[37] Finally, f can be estimated from eq 7 with measurements of the transdermal resistance drop induced by ultrasound. The estimation of f is described in detail in the next section.

Estimation of f—As just mentioned, f can be estimated from the experimentally measured drop in the electrical resistance of the skin upon application of ultrasound. Equation 7 predicts that if the entire lipid bilayer region is disordered (that is, if $f \approx 1$), the electrical resistance of the skin should drop by a factor of ~8. Accordingly, to ascertain whether eq 7 represents the phenomenon of bilayer structural disordering correctly, we performed the following experiments.

We measured the electrical resistance of the skin during a long (7 h) exposure to ultrasound. As described earlier, a continuous application of ultrasound causes deaerating of the solutions, thus making further exposure to ultrasound ineffective. To overcome this problem, we aerated the donor and receiver solutions every hour. The variation in R/R_o with time is shown in Figure 11. The electrical resistance decreases upon ultrasound exposure and tends to plateau after ~45 min (this plateau is not seen clearly in Figure 11; for a clearer view of this plateau, see Figure 5). However, after aerating again (see the *Experimental Section* for a discussion of the aerating methods), the electrical resistance further decreases significantly. This result is consistent with our initial observations that the procedure of aerating every hour maintains the effect of ultrasound on estradiol permeability coefficient at a high value. This observation that the repeated aerating procedure maintains the effect of ultrasound on the skin electrical resistance at a high value provides additional support to the hypothesis that cavitation occurs inside the SC. Another feature of the variation of the electrical resistance shown in Figure 11 is that the effect of repeated aerating decreases with time and reaches a plateau corresponding to a drop of resistance by a factor of 5 ± 1.5. This observation

is in close agreement with the prediction of eq 7 that the maximum decrease in electrical resistance should approach a factor of 8. This finding supports the use of eq 7 to represent the structural changes that take place in the SC during ultrasound exposure.

The fraction of lipid bilayer disordered due to ultrasound exposure depends significantly on the number of aerations. In the permeation experiments, we aerated the donor and receiver solutions every 4 h. Hence, in most of our permeation experiments, total disordering of the lipid bilayers did not occur. To estimate the fraction of the lipid bilayers disordered in our permeation experiments, we performed additional electrical resistance measurements under exactly the same conditions as those corresponding to the permeation experiments discussed in the *Experimental Section* (ultrasound frequency, 1 MHz; intensity, 1 W/cm^2; donor and receiver solutions aerated every 4 h). Typically, the electrical resistance dropped to ~60% (± 10%) of its initial value over the duration of an experiment. It is important to note that the skin electrical resistance may also drop because of the increase in skin temperature. In a different set of experiments (results not shown) the resistance dropped by ~14% when the skin temperature increased by 7 °C (a typical increase in the skin temperature during our sonophoresis experiments), suggesting that 14% of the skin resistance drop upon ultrasound exposure may be attributed to thermal effects. However, because the contribution of thermal effects to ultrasonic permeation enhancement has been neglected in the derivation of eq 6, we also attribute the entire electrical resistance drop to cavitational effects. Substitution of $\bar{\sigma}/\bar{\sigma}^{us} = 0.6$ (±0.1) in eq 7 results in a value of $f = 0.13 \pm 0.05$. This value suggests that only ~13% of the lipid bilayer region surrounding the keratinocytes is disordered by the cavitation bubbles generated during the therapeutic ultrasound application. This small fraction of disordered bilayers also suggests that cavitation probably occurs in the keratinocytes of the SC. If any significant cavitation had occurred in the intercellular lipids, one would expect that a much larger fraction of the lipids should be disordered.

Comparison with Experimental Data of Sonophoresis: Dependence of Sonophoresis on Permeant Characteristics—Equation 6 suggests that the ultrasonic enhancement of transdermal molecular transport varies from one permeant to another. Specifically, the transport of permeants that are capable of passively diffusing through the skin rapidly (i.e., with a lipid–bilayer diffusion coefficient, D_o, nearly equal to the disordered bulk diffusion coefficient, D^∞), should be least affected by the application of ultrasound. On the other hand, permeants that passively diffuse through the skin very slowly are most susceptible to ultrasonic enhancement.

The theoretically predicted as well as the experimentally measured values (circles) of the ultrasonic transdermal transport enhancement, E, as a function of the ratio D^∞/D_o, are shown in Figure 12. The theoretical predictions in Figure 12 correspond to the shaded region between two lines obtained by substituting $f = 0.18$ (upper line) or $f = 0.08$ (lower line) in eq 6; that is:

$$E = (1 - f) + f\left[\frac{D^\infty}{D_o}\right]$$

Values of D_o and D^∞ for various permeants are listed in Table 1 (see the footnote in Table 1 for a discussion of the estimation of D_o). The bulk diffusion coefficient of a permeant, D^∞, is assumed to be the diffusion coefficient in free hydrocarbon (in this case, octane) and is estimated with the empirical formula described in ref 37.

The agreement between theory and experiment shown in Figure 12 is especially significant because no fitted parameters

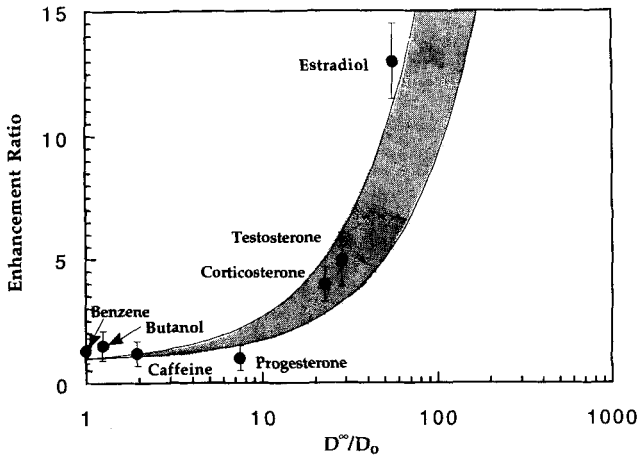

Figure 12—Comparison of the theoretically predicted ultrasound-mediated transdermal transport enhancement values, E (solid lines indicate the upper and the lower limits on the theoretical predictions), and the experimentally measured values (circles) plotted against the ratio D^∞/D_o.

are used in the theoretical predictions. As predicted by eq 6, the molecules diffusing passively at a fast rate (e.g., benzene) are unaffected by ultrasonic exposure, whereas those diffusing slowly (e.g., estradiol) are significantly affected. These findings have important consequences regarding the efficacy of therapeutic ultrasound-mediated transdermal drug delivery. *The results indicate that the slower the diffusion of a permeant through the lipid bilayers of the SC (as reflected by its low D_o value), the more effective is ultrasound in enhancing its transport.* It is noteworthy that because the skin permeability to a compound is governed by its partition coefficient as well as by its diffusion coefficient, the slowest *permeating* molecules are not necessarily the slowest *diffusing* ones. For example, the permeability coefficient of caffeine is one order of magnitude smaller than that of estradiol (see Table 1). Nevertheless, caffeine diffuses through the lipid bilayers of the SC at a rate that is two orders of magnitude higher than estradiol (compare the passive diffusion coefficient values listed in Table 1 for the two permeants). Accordingly, whereas caffeine permeates more slowly through the SC than estradiol, ultrasound is more effective at enhancing the permeation of estradiol.

Conclusions—Various phenomena, including cavitation, thermal effects, generation of convective velocities, and mechanical effects, have been analyzed as possible mechanisms of sonophoresis. Cavitation-induced lipid bilayer disordering was found to be the most important cause for ultrasonic enhancement of transdermal transport. The observed enhancement depends significantly on the chemical nature of the permeant. A theoretical model was developed to predict sonophoretic transdermal transport enhancement. The theoretical predictions, as well as the measured sonophoretic enhancement for different permeants, suggest that the drugs passively diffusing through the skin at a slow rate are most enhanced by the application of ultrasound. These findings provide quantitative guidelines for estimating the efficacy of sonophoresis in enhancing transdermal drug delivery.

References and Notes

1. Bronaugh, R. L.; Maibach, H. I., Eds.; *Percutaneous Absorption: Mechanisms-Methodology-Drug Delivery*; Marcel Dekker: New York, 1989; pp 1–12.
2. Jarrett, A., Ed.; *The Physiology and Pathology of the Skin*; Academic: London, 1978; Vol. 5.
3. Flynn, G. L., In *Percutaneous Absorption: Mechanisms-Methodology-Drug Delivery*; Mercel Dekker: New York, 1989; pp 27–51.

4. Burnette, R. R. In *Developmental Issues and Research Initiatives*; Hadgraft, J.; Guy, R. H., Eds.; Marcel Dekker: New York, 1989; pp 247–288.
5. Prausnitz, M. R.; Bose, V.; Weaver, J. C.; Langer, R. *Proc. Natl. Acad. Sci. U.S.A.* **1993**, *90*, 10504–10508.
6. Walters, K. A. In *Transdermal Drug Delivery: Developmental Issues and Research Initiatives*; Hadgraft, J.; Guy, R. H., Eds.; Marcel Dekker, New York, 1989.
7. Kost, J.; Levy, D.; Langer, R. *Proc. Int. Symp. Control. Rel. Bioact. Mater. 13*; Controlled Release Society: 1986; pp 177–178.
8. Levy, D.; Kost, J.; Meshulam, Y.; Langer, R. *J. Clin. Invest.* **1989**, *83*, 2074–2078.
9. Bommanan, D.; Menon, G. K.; Okuyama, H.; Elias, P. M.; Guy, R. H. *Pharm. Res.* **1992**, *9*, 559–564.
10. Bommanan, D.; Menon, K.; Okuyama, H.; Elias, P. M.; Guy, R. H. *Pharm. Res.* **1992**, *9*, 1043–1047.
11. Menon, G. K.; Bommanan, D. B.; Elias, P. M. *Skin Pharmacol.* **1994**, *7*(3), 130–139.
12. Tachibana, K.; Tachibana, S. *Anesthesiology* **1993**, *78*, 1091–1096.
13. Miyazaki, S.; Mizuoka, H.; Oda, M. *J. Pharm. Pharmacol.* **1991**, *43*, 115–116.
14. Benson, H. A. E.; McElnay, J. C.; Hadgraft, J. *Pharm. Res.* **1991**, *8*, 204–209.
15. The diffusion coefficient, D, of a typical permeant in water is $\sim 1 \times 10^{-5}$ cm^2/s (estimated using the Wilke–Chang equation described in ref 37). The lower limit on the boundary-layer permeability, P, can then be estimated by assuming that the boundary-layer thickness is equal to the length of the diffusion cell (l = 2 cm). This lower limit was estimated to be ~0.02 cm/h ($P = D/l$). Note that the actual boundary-layer permeability may be >1000 times higher than this low limit because of stirring. The measured skin permeabilities, except for benzene, are significantly lower than 0.02 cm/h (see Table 1), thus suggesting that the boundary-layer resistance is small compared with the skin-permeation resistance.
16. Rozenberg, L. D. *Physical Principles of Ultrasonic Technology*; Plenum: New York, 1973; Vol. 1, pp 379–496.
17. Davies, R., Ed.; *Cavitation in Real Liquids*; American Elsvier: New York, 1964.
18. Crum, L. *Nature (London)* **1979**, *278*, 148.
19. Gaertner, W. *J. Acoust. Soc. Am.* **1954**, *26*, 977–980.
20. Suslick, K. S. *Ultrasound: Its Chemical, Physical, and Biological Effects*; VCH Publishers: New York, 1989; pp 287–301.
21. Crum, L. A.; Folwlkes, J. B. *Nature* **1986**, *52*, 319.
22. Frizzel, L. A.; Lee, C. S.; Aschenbach, P. D.; Borreli, M. J.; Morimoti, R. S.; Dunn, F. J. *Acoust. Soc. Am.* **1983**, *74*, 1062.
23. Apfel, R. E. *IEEE Trans. Ultrason. Ferroelectrics Freq. Control* **1986**, *UFFC-33*, 139.
24. Nyborg, W. L. In *Physical Acoustics*; Mason, W. P., Ed.; Academic: New York, 1965; Vol. 2B, pp 265–283.
25. Bergemann, L. In *Ultrasound: Physical, Chemical, and Biological Effects*; El'piner, I. E., Ed.; Consultants Bureau: New York, 1964.
26. Knutson, K.; Krill, S. L.; Lambert, W. J.; Higuchi, W. I. *J. Controlled Release* **1987**, *6*, 59–74.
27. Allenby, A.; Fletcher, J.; Schok, C.; Tees, T. F. S. *Br. J. Dermatol.* **1969**, *81*, 31–62.
28. Bird, R. B.; Stewart, W. E.; Lightfoot, E. N. *Transport Phenomena*; John Wiley & Sons: New York, 1960; pp 130–132.
29. Van Krevelen, D. W. *Properties of Polymers, Their Estimation and Correlation with Chemical Structure*; Elsevier: New York, 1976.
30. Elias, P. M. *Drug Dev. Res.* **1988**, *13*, 97–105.
31. Bodde, H. E.; Homan, B.; Spies, F.; Weerheim, A.; Kempenaar, J.; Ponec, M. *J. Invest. Dermatol.* **1990**, *95*, 108–116.
32. Edwards, D. A.; Langer, R. *J. Pharm. Sci.* **1994**, *83*, 1315–1334.
33. Faxen, H. *Ann. Phys.* **1992**, *68*, 89–95.
34. Glandt, E. D. *AIChE J.* **1981**, *27*, 51–59.
35. Bouwasta, J. A.; de Vries, M. A.; Gooris, G. S.; Bras, W.; Brussee, J.; Ponec, M. *J. Controlled Release* **1991**, *15*, 209–220.
36. Diamond, J. M.; Katz, Y. *J. Membr. Biol.* **1974**, *17*, 121.
37. Perry, R. H.; Green, D. W. *Chemical Engineering Handbook*; 5th ed.; McGraw-Hill Book: New York, 1973; pp 3–286.

Acknowledgments

We thank Ashish Patel for technical assistance, Mark Johnson for insightful comments, and Professor Joseph Kost for helpful discussions. We also thank David Smith for assistance in performing the confocal microscopy studies. This work was supported by the National Institute of Health (NIH grant GM44884). DB acknowledges the support of the National Science Foundation (NSF) Presidential Young Investigator award.

JS940639Z